Corrosion in heat exchangers in geothermal power plants

Willem Faes[1,2], Steven Lecompte[1], Johan Van Bael[2,3], Robbe Salenbien[2,3], Kim Verbeken[4], Michel De Paepe[1,5]

[1] Department of Flow, Heat and Combustion Mechanics, Ghent University, Ghent, Belgium
[2] Flemish Institute of Technological Research (VITO), Mol, Belgium
[3] EnergyVille, Thor Park, Genk, Belgium
[4] Department of Materials, Textiles and Chemical Engineering, Ghent University, Ghent, Belgium
[5] Flanders Make, core lab UGent-EEDT, www.flandersmake.be

willem.faes@ugent.be

Keywords: corrosion, heat exchangers, geothermal, modelling, experimental.

ABSTRACT

In geothermal power plants that use low to medium temperature geothermal reservoirs, electricity is generated using an organic Rankine cycle or heat is provided to district heating networks. The energy in the geothermal fluid is recovered with a heat exchanger. Since the temperatures and pressures are relative high (100-150°C, 40 bar), metallic heat exchangers are preferred. These are however susceptible to corrosion in the aggressive geothermal environment, so highly corrosion resistant materials should be used or suitable coatings should be applied. This has an adverse impact on the financial viability of the project. Therefore, this research investigates the possibility to use cheaper materials that come in contact with the brine. First, a model is described to determine the total cost of ownership of the heat exchanger and to determine an optimal design. Additionally, an experimental setup is described. This setup will allow to calibrate the corrosion parameters implemented in the model, to determine the influence of corrosion on the performance of the heat exchanger and to assess the influence of the flowing conditions on the corrosion process. In this paper, the methodology and expected outcome are described.

1. INTRODUCTION

Currently in Belgium, the application of geothermal energy is limited to mainly shallow geothermal utilization with ground source heat pumps (GSHP) with an installed capacity of 198.7 MWt (Berckmans and Vandenberge, 1998). It was however calculated that an aquifer in the Campine basin has a potential of 13.02×10^9 GJ (GEOHEAT-APP, 2014), providing an interesting alternative to polluting fossil fuels. One pilot project was therefore initiated by VITO (the Flemish Institute of Technological Research), who succeeded in drilling into the aquifer and delivering geothermal brine with a temperature of 128°C. This brine has up to 165 g/l total dissolved ions (mainly sodium and chloride) and is saturated with carbon dioxide (CO_2). This causes the brine to be corrosive to metals which are exposed to it (Faes et al., 2019). However, because of the high temperatures and since the pressure in the pipes and installations can reach 40 bar, metals are the preferred construction material.

One specific piece of equipment for which this is problematic, is the heat exchanger. It has been shown before that corrosion can reduce the thermohydraulic performance and hinder safe operation (Faes et al., 2019). One solution could be to use extremely corrosion resistant materials such as titanium or highly alloyed steel types. These are however problematic regarding machinability and weldability and the investment cost increases significantly. It has been calculated before that this has a strong impact on the profitability of the geothermal project (Walraven et al., 2015).

In this study the possibility of employing cheaper materials in the construction of the heat exchanger, like e.g. carbon steel, is investigated. It might be demonstrated to be more economic to use a well-designed carbon steel heat exchanger and replace it several times over its lifetime (because of a too large degree of corrosion) than to employ a titanium heat exchanger.

For that reason, a heat exchanger design optimization model is created. This model, focusing on shell-and-tube heat exchangers, is based on existing design optimization models, which can amongst other be found in the publications by Selbaş et al. (2006), Caputo et al. (2008) and Sanaye and Hajabdollahi (2010). For a more thorough survey of the existing work, the reader is referred to the review paper by Gosselin (2009).

To be able to take scaling and corrosion into account, this design model is extended with a corrosion and maintenance model. An experimental setup was built to evaluate and calibrate this model and is discussed further in this paper.

2. DESIGN OPTIMIZATION MODEL

Because of the high powers (7 MW) and mass flow rates (40 kg/s) expected in the geothermal power plant, in combination with a high pressure (40 bar), this study focusses on shell-and-tube heat exchangers. An example of such a device can be seen in Figure 1. It consists of a number of tubes inside a shell. Since the brine is corrosive, it will flow inside the tubes. To direct the secondary fluid (water) over the tubes, a number of baffles are inserted inside the shell.

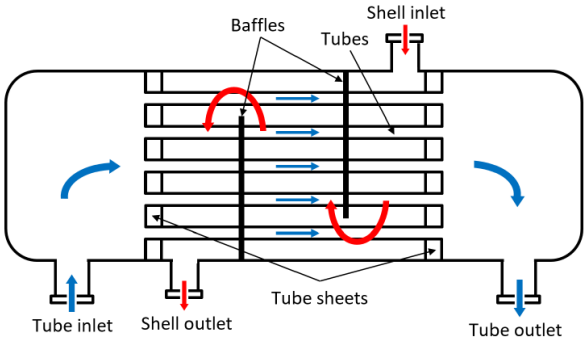

Figure 1: Schematic representation of a shell-and-tube heat exchanger.

During the design of the heat exchangers, there is always a trade-off between heat transfer rates and pressure drop. This design optimization model will determine the design that has the lowest total cost of ownership (TCO, explained further) over the entire lifetime of the power plant.

Similar to the work of Selbaş et al. (2006), Caputo et al. (2008) and Sanaye and Hajabdollahi (2010), a set of equations determining these heat transfer rates and pressure drop for a certain heat exchanger design is at the basis of this model. In the present study the heat exchanger is thermally modelled using the ε-NTU method. The effectiveness of the heat exchanger (a TEMA E type shell) was estimated from (Kakaç, 2002):

$$\varepsilon = \frac{1-\exp\left(-NTU\cdot(1-C^*)\right)}{1-C^*\cdot\exp\left(-NTU\cdot(1-C^*)\right)} \quad [1a]$$

for 1 tube pass and

$$\varepsilon = \frac{2}{1+C^*+(1+C^{*2})^{\frac{1}{2}}\cdot\frac{1+\exp\left(-NTU\cdot(1+C^{*2})^{\frac{1}{2}}\right)}{1-\exp\left(-NTU\cdot(1+C^{*2})^{\frac{1}{2}}\right)}} \quad [1b]$$

for multiple tube passes.

In this equation, the number of transfer units (NTU) and the heat capacity rate ratio (C^*) are given in the following equations

$$NTU = \frac{A_o\cdot U_o}{C_{min}} \quad [2]$$

$$C^* = \frac{C_{min}}{C_{max}} = \frac{(\dot{m}\cdot c_p)_{min}}{(\dot{m}\cdot c_p)_{max}} \quad [3]$$

Where A_o is the heat transfer surface area, U_o is the overall heat transfer coefficient, $\dot{m}$ the mass flow rate and c_p the specific heat capacity. A_o and U_o are calculated as follows:

$$A_o = \pi\cdot d_o\cdot N_t\cdot L \quad [4]$$

$$U_o = \frac{1}{\frac{1}{h_s}+R_{of}+d_o\cdot\frac{\ln\left(\frac{d_o}{d_i}\right)}{2\cdot k_m}+R_{if}\cdot\frac{d_o}{d_i}+\frac{1}{h_t}\cdot\frac{d_o}{d_i}} \quad [5]$$

Here, d_o and d_i are the outer and inner tube diameter, N_t is the number of tubes, L is the tube length, h_s and h_t are the heat transfer coefficient on the shell and tube side, R_{of} and R_{if} are the outer and inner fouling factors and k_m is the metal thermal conductivity. The calculation of the heat transfer coefficient and the pressure drop on either side of the tubes are explained next.

2.1 Tube side performance

The equations used to determine the heat transfer coefficient inside the tubes is dependent on the flow regime (indicated by the Reynolds number, Re_t) and given in the following equations:

$$h_t = \frac{\lambda}{d_i}\cdot\left[3.657+\frac{0.0677\cdot\left(Re_t\cdot\mathrm{Pr_t}\cdot\frac{d_i}{L}\right)^{1.33}}{1+0.1\cdot Pr_t\cdot\left(Re_t\cdot\frac{d_i}{L}\right)^{0.3}}\right] \quad [6a]$$

$Re_t < 2300$; Stephan and Preuβer (Lee et al. 2005)

$$h_t = \frac{\lambda}{d_i}\cdot\left[\frac{\frac{f_t}{8}\cdot(Re_t-1000)\cdot Pr_t}{1+12.7\cdot\sqrt{\frac{f_t}{8}}\cdot(Pr_t^{0.67}-1)}\cdot\left(1+\left(\frac{d_i}{L}\right)^{0.67}\right)\right] \quad [6b]$$

$2300 < Re_t < 10^4$; Gnielinski (Lee et al., 2005)

$$h_t = \frac{\lambda}{d_i}\cdot 0.027\cdot Re_t^{0.8}\cdot Pr_t^{\frac{1}{3}} \quad [6c]$$

$Re_t > 10^4$; Sieder and Tate (Kern, 1950)

In the previous equations, λ and Pr_t are the thermal conductivity and the Prandtl number of the fluid, Re_t is the Reynolds number inside the tubes and f_t is the Darcy friction factor. This friction factor is calculated as using the Gnielinski correlation (Lee et al., 2005):

$$f_t = (1.82\cdot\log(Re_t)-1.64)^{-2} \quad [7]$$

The same friction factor is used in the calculation of the tube side pressure drop (Kakaç, 2002):

$$\Delta P_t = \frac{\rho\cdot v_t}{2}\cdot\left(f_t\cdot\frac{L}{d_i}+4\right)\cdot N_p \quad [8]$$

2.2 Shell side performance

The Bell-Delaware method is used to determine the heat transfer coefficient and pressure drop on the shell side.

For the calculation of the heat transfer coefficient h_s, this method starts with the calculation of the heat transfer coefficient for pure crossflow of an ideal tube-

bank, h_{id} (Equation 9) (Kuppan, 2013). Next, several correction factors, J, are applied to take bypass flows into account (Equation 10). For the calculation of these correction factors, the reader is referred to the book of Kuppan (2013).

$$h_{id} = \frac{j_i \cdot c_{p,s} \cdot G_s}{Pr_s^{\frac{2}{3}}} \cdot \left(\frac{\phi_s}{\phi_w}\right)^{0.14} \quad [9]$$

$$h_s = h_{id} \cdot J_c \cdot J_l \cdot J_b \cdot J_s \cdot J_r \quad [10]$$

In Equation 9, $c_{p,s}$ is the specific heat capacity of the fluid on the shell-side, G_s is the mass velocity on the shell-side, Pr_s is the Prandtl number on the shell side and μ_s and μ_w are the dynamic viscosity at the shell-side temperature and at wall temperature. The ideal Colburn j factor is represented by j_i. The reader is again referred to the book of Kuppan (2013) for the calculation of this factor.

2.3 Cost estimation

In the calculation of the TCO of the heat exchanger, both the investment cost and the operational costs are taken into account. The investment cost, C_{inv} (USD), is determined with the method by Hall (1982), explained in the work of Taal (2003). The calculation of the heat exchanger cost, done with Equation 11, is dependent on the heat transfer surface area A (m²) and the construction material. The coefficients used in this equation are given in Table 1.

$$C_{inv} = C_1 + C_2 \cdot A^{C_3} \quad [11]$$

Table 1: Coefficients used to calculate the heat exchanger investment cost with Equation 11, (Taal, 2003).

Material (shell-tube)	C_1	C_2	C_3
Carbon steel (CS) – CS	7000	360	0.8
CS – stainless steel (SS)	8500	409	0.85
SS – SS	10000	324	0.91
CS – titanium (Ti)	14000	614	0.92
Ti – Ti	17500	699	0.93

The discounted operational costs for month n, C_{opD}, are based on the pumping power, P, with the following approach:

$$P = \frac{\Delta P_t \cdot V_t}{\eta_t} + \frac{\Delta P_s \cdot V_s}{\eta_s} \quad [12]$$

$$C_{op} = P \cdot c_E \cdot T \quad [13]$$

$$C_{opD} = \frac{C_{op}}{(1+i_m)^n} \quad [14]$$

Where V_t and V_s are the pressure drop over the tubes and the shell, η_t and η_s are the pump efficiencies, c_E is the price of electricity, T is the duration of the period during which the operational costs are calculated, i_m is the monthly interest rate and n represents the number of the current month.

2.4 Design optimization

Several optimization algorithms have been created for the optimisation of the design of shell-and-tube heat exchangers in literature (Gosselin, 2009). In this study, it was chosen to use a genetic algorithm (GA), which has been proven be effective and has a low computational time (Selbas, 2006).

GA's start from an initial population of randomly created individuals (heat exchanger designs). These individuals are chosen within several constraint. The TCO of all these individuals is calculated and a subsequent population is created using the principles of survival of the fittest. Each subsequent generation should contain better performing (i.e. a lower TCO) than the previous presentation. Each new generation is created with the following GA rules:

- The best individuals are copied to the next generation.
- New child individuals are obtained by selecting a pair of parents in the current generation and crossover of their genes.
- Mutations of selected individuals.

3. CORROSION AND MAINTENANCE MODEL

Existing investigations on the design of heat exchangers solely focus on finding the optimal design for a fixed exchanger performance (Selbaş et al., 2006, Caputo et al., 2008 and Sanaye and Hajabdollahi, 2010). According to the author's knowledge, no studies exist taking into account varying performances of the heat exchanger caused by corrosion, scaling or fouling. Furthermore, all existing studies consider a constant price of electricity and constant mass flow rates and assume that the heat exchanger will be able to operate for an indefinite amount of time.

In this study, varying conditions can be applied. Additionally, a corrosion and maintenance model has been implemented. This corrosion model assumes that the inside of the tubes corrodes uniformly. With this model, a small decay in thickness of the tubes, with possibly a formation of a corrosion layer is applied monthly. The performance and operational cost are calculated accordingly, since a change in diameter, surface roughness and thermal conductivity of the wall will influence the heat transfer coefficient and the pressure drop, in a similar way as would fouling (see Figure 2). A change in behaviour of the corrosion rate and formation of the corrosion scale can be imposed depending on the flow velocity inside the tubes.

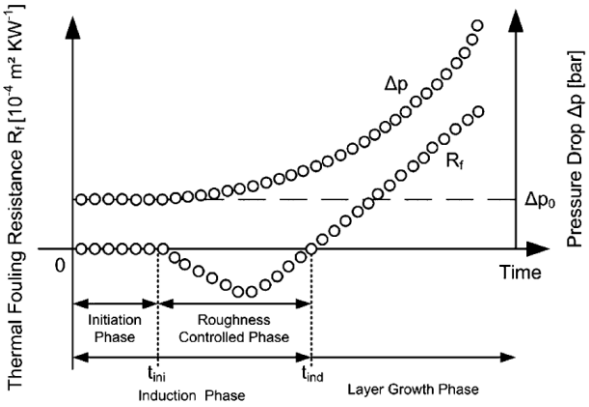

Figure 2: Evolution of thermal fouling resistance and pressure drop for precipitation fouling (Schoenitz et al., 2015).

This decay in performance would cause the operators of a geothermal power plant to react when it has advanced too much. Two possible actions were included in the model, depending on the state of the heat exchanger. If there is either an unacceptable increase in pressure drop or decrease in heat transferred, while the remaining wall thickness of the tubes is still sufficient to withstand the pressure, a cleaning action is simulated. The scaling thickness is reset to zero and the surface roughness is reduced to its original value and a (discounted) cost for cleaning is added to the operational cost of the respective month. It is also possible that the remaining wall thickness has reduced below a certain threshold. In that case, the heat exchanger is replaced by a new one with the original dimensions and a (discounted) cost of purchase is added to the investment cost.

At the time of writing, only preliminary results have been obtained without performing an optimization. In Figure 3, the cumulative costs of two heat exchangers, calculated with the model, are illustrated. The first heat exchanger (HEX 1) represents a titanium shell-and-tube heat exchanger with a relatively low pressure drop that is not susceptible to corrosion. The same design and operational conditions are used for the second heat exchanger (HEX 2), so approximately the same operational costs are obtained. This heat exchanger is however constructed of carbon steel. A uniform corrosion rate of 0.3 mm/year was assumed and the corrosion products are defined to be twice as voluminous as the base metal. Additionally, a maximal velocity in the tubes of 2 m/s and a maximal scale thickness of 1 mm were imposed. The heat exchanger is in this example replaced when the tube wall thickness drops below 0.5 mm (no cleaning operations). For the lifetime of the power plant, a period of 20 years was taken. This first case exemplifies that it would be more economic to replace a carbon steel heat exchanger twice than to use an expensive titanium heat exchanger.

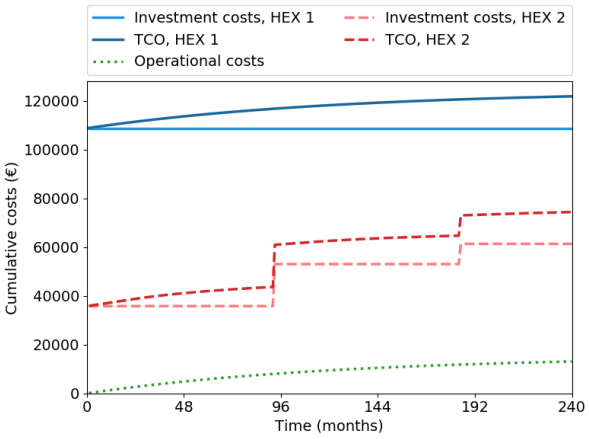

Figure 3: Cumulative cost for a titanium heat exchanger (HEX 1) and a carbon steel heat exchanger (HEX 2).

The input given for the corrosion model in the previous simulation is currently only estimated based on initial measurements of the material in a static brine. The behaviour of this steel is expected to differ significantly in an operational heat exchanger. Also on the behaviour of the corrosion products (e.g. dissolve in the brine or form a scale), little is known. Therefore, an experimental setup is being built.

4. EXPERIMENTAL SETUP

To be able to accurately determine the corrosion rate inside a tube with flowing geothermal brine and to estimate the influence of the corrosion (and corrosion fouling) on the heat transfer performance, an experimental setup was build. The setup has a design similar to that of an apparatus discussed by Knudsen (1981) to measure fouling resistances. It consists of a double pipe heat exchanger, where the artificial geothermal brine flows inside the tube and a cooling fluid in the annulus. The brine is heated up to maximally 90°. Experiments at temperatures above the boiling point of the brine are not possible because of technical constraints. These limitations arise from the fact that for most components and installation parts, plastic constructions materials have been chosen to avoid corrosion of these parts and galvanic corrosion effects between metallic parts and the test section. A schematic layout of the setup is given in Figure 4.

The tube in test section has a length of 2 m, an internal diameter of 8 mm and a thickness of 2 mm. This tube is made of carbon steel (alloy S235JR) with a thermal conductivity of approximately 52 W/m.K. The brine will enter at a temperature of 80°C and saturated with CO_2 with a velocity of 1.2 m/s. At the cooling water side, water will enter with a temperature of 20°C. A heat transfer of approximately 4 kW will be achieved.

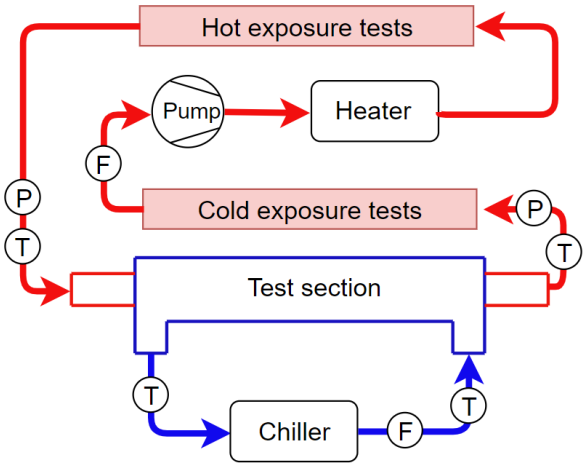

Figure 4: Schematic representation of the test setup, with indication of the temperature (T), pressure (P) and flow rate (F) sensors.

The setup has been equipped with several sensors (see Figure 4) to monitor the performance of the heat exchanger and to assess the ability of the sensing technique to determine the degree of corrosion or fouling.

In both the brine loop and the cooling loop, temperature sensors have been placed before and after the test section. Together with measurements of mass flow rates on either side, the heat transfer rate can be determined.

In addition to the temperature measurements, the brine loop has been equipped with pressure sensors. Variations in pressure drop over the test section should allow to detect a change in surface roughness or internal diameter.

Finally, by the use of a handheld ultrasonic thickness gauge, the wall thickness of the corroding tube will be monitored. Measurements are possible before and after the test section, so an assessment of the influence of temperature is possible.

In addition to the measurements performed on the test section, short pieces of the same tube (approx. 6 cm), have been connected in series before and after the test section. By weighing the pieces before exposure to the brine and after a certain period of measurements (e.g. 1 month), a uniform corrosion rate (CR) can be calculated with equation 15. In this equation, Δm is the mass loss, A is the exposed material surface area, ρ is the material density, T is the exposure period and K is a constant to determine the unit (e.g. mm/y). This method is based on the ASTM G1 Standard (ASTM, 2003). Similar tests have already been done in static conditions. Results from both type of experiments will be compared to determine the influence of the flowing conditions on the corrosion process.

$$CR = \frac{\Delta m \cdot K}{A \cdot \rho \cdot T} \qquad [15]$$

The values obtained with these measurements can also be used to evaluate the suitability of using the ultrasonic thickness sensor. According to Equation 16, The measured reduction, Δt, in thickness should equal the one calculate with Equation 15.

$$\Delta t = t_o - t_i = CR \cdot T \qquad [16]$$

Finally, the corroded inside of the tube will be examined with microscopic techniques. The investigation of a cross section will demonstrate the reduction in thickness of the base metal and the thickness of the corrosion layer. Measurements with X-ray diffraction (XRD) or X-ray photoelectron spectroscopy (XPS) will allow to determine the composition of the formed scale. By the experience gained with previous measurements in static conditions, an iron carbonate scale ($FeCO_3$) is expected. Also the surface roughness will be determined. The information gathered from the measurements after the experiments will allow to fine-tune the parameters used in the corrosion model.

At the time of writing, first measurement campaign has just started, so no results of corrosion tests in flowing conditions have been obtained yet.

5. CONCLUSIONS

In this paper, a methodology to determine a heat exchanger design with a minimal total cost of ownership for a geothermal powerplant is explained.

In a first part the heat exchanger optimization is discussed. This model calculates the thermohydraulic performance and cost of a heat exchanger when operational conditions and a certain design are given. A genetic algorithm is used to search for optimal design.

Next, a corrosion and maintenance model, implemented in the heat exchanger model, is discussed. This corrosion model describes the behaviour of the base metal and the corrosion layer over time for different temperatures and flow velocities. With the maintenance model, cleaning of a heat exchanger with reduced performance or replacement of a heat exchanger where corrosion has excessively advanced is simulated. Some first results of this model are shown. These are however preliminary, since the knowledge on the corrosion process is insufficient.

To determine the correct parameters for the corrosion model, to investigate the influence of corrosion on the performance of the heat exchanger and to investigate the influence of the flowing conditions on the corrosion process, an experimental setup was built. This setup is described in the last section. A test section is included consisting of a double pipe heat exchanger. The inside surface of the smaller pipe will corrode because of the flowing geothermal brine. In addition to the test section, small tube samples are installed in series to perform exposure tests. Results of these tests will be compared to results from tests in static conditions. However, at the time of writing, no results of tests in flowing conditions have been obtained yet.

REFERENCES

ASTM: Standard G1-03: Standard practice for preparing, cleaning and evaluating corrosion test specimens, *American Society for Testing and Materials*, (2003).

Berckmans, A. and Vandenberghe, N.: Use and potential of geothermal energy in Belgium, *Geothermics 27(2)*, (1998), 235-242.

Caputo, A.C., Pacifico, M.P., and Paolo, S.: Heat exchanger design based on economic optimisation, *Applied thermal engineering*, 28.10, (2008), 1151-1159.

Faes, W., Lecompte, S., Ahmed, Z.Y., Van Bael, J., Salenbien, R., Verbeken, K. and De Paepe, M., Corrosion and corrosion prevention in heat exchangers, *Corrosion reviews*, (2019).

Faes, W., Lecompte, S., Van Bael, J., Salenbien, R., Bäβler, R., Bellemans, I., Cools, P., De Geyter, N., Morent, R., Verbeken, K. and De Paepe, M.: Corrosion behaviour of different steel types in artificial geothermal fluids, *To be published*, (2019).

GEOHEAT-APP: Economical feasibility of deep and intermediary geothermal energy in supplying sustainable heat for new building and renovation projects, *VITO, Grontmij Nederland & TNO, Iva*, 2014.

Gosselin, L., Tye-Gingras, M., Mathieu-Potvin, F.: Review of utilization of genetic algorithms in heat transfer problems, *International Journal of Heat and Mass Transfer*, 52.9-10, (2009), 2169-2188.

Hall, R.S., Matley, J., and McNaughton, K.J.: Current Costs of Process Equipment, *Chemical Engineer*, 89.7, 1982, 80-83.

Kakaç, S, Liu, H, and Pramuanjaroenki, A.: Heat exchangers: selection, rating, and thermal design, *CRC press*, 2002.

Kern, D.Q.: Process heat transfer, *Tata McGraw-Hill Education*, 1950.

Knudsen, J.G.: Apparatus and techniques for measurement of fouling of heat transfer surfaces, *Fouling of heat transfer equipment*, (1981), 57-81.

Kuppan, T..: Heat exchanger design handbook, *CRC press*, 2013.

Lee, P.S., Garimella, S.V. and Liu, D.: Investigation of heat transfer in rectangular microchannels, *International Journal of Heat and Mass Transfer*, 48.9, (2005), 1688-1704.

Sanaye, S., and Hajabdollahi, H.: Multi-objective optimization of shell and tube heat exchangers, *Applied Thermal Engineering*, 30.14-15, (2010), 1937-1945.

Schoenitz, M., Grundemann, L., Augustin, W., and Scholl, S.: Fouling in microstructured devices: a review, *Chemical Communications*, Vol. 51, (2015), 8213-8228.

Selbaş, R., Önder K., and Marcus R.: A new design approach for shell-and-tube heat exchangers using genetic algorithms from economic point of view, *Chemical Engineering and Processing: Process Intensification*, 45.4, (2006), 268-275.

Taal, M., Bulatov, I., Klemeš, J., & Stehlík, P.: Cost estimation and energy price forecasts for economic evaluation of retrofit projects, *Applied thermal engineering*, 23(14), (2003), 1819-1835.

Walraven, D., Laenen, B. and D'haeseleer, W.: Minimizing the levelized cost of electricity production from low-temperature geothermal heat sources with ORCs: Water or air cooled?, *Applied Energy*, vol. 142, (2015), 144-153.

Acknowledgements

This work was done with the support of the EU, ERDF, Flanders Innovation & Entrepreneurship and the Province of Limburg.